Check for updates

Global Ecology and Biogeography

WILEY

Global Ecology and Biogeography | A Journal of Macroecology

RESEARCH ARTICLE OPEN ACCESS

Mountain Roads Across the Globe Significantly Alter Local Soil Thermal Microclimates

Renée Lejeune[1,2] | Eduardo Fuentes-Lillo[3,4] | Jake Alexander[5] | Romina D. Dimarco[6] | Stef Haesen[7,8] | Sylvia Haider[9] | Lore Hostens[10] | Anke Jentsch[11] | Josef Kutlvašr[12,13] | Jonathan Lenoir[14] | Martin A. Nuñez[6] | Aníbal Pauchard[3,4] | Jan Pergl[12] | Amber Pirée[1] | Amanda Ratier Backes[15] | Tim Seipel[16] | Michaela Vítková[12] | Dymphna Wiegmans[1] | Peter Wolff[11] | Ivan Nijs[1] | Jonas J. Lembrechts[1,17]

[1]Plants & Ecosystems, Department of Biology, University of Antwerp, Antwerp, Belgium | [2]Conservation Biology, Department of Ecology, Sveriges Lantbruksuniversitet, Uppsala, Sweden | [3]Laboratorio de Invasiones Biológicas, Facultad de Ciencias Forestales, Universidad de Concepción, Concepción, Chile | [4]Institute of Ecology and Biodiversity (IEB), Santiago, Chile | [5]Institute of Integrative Biology, ETH Zurich, Zurich, Switzerland | [6]Department of Biology and Biochemistry, University of Houston, Houston, Texas, USA | [7]Department of Earth and Environmental Sciences, Leuven, Belgium | [8]KU Leuven Plant Institute, KU Leuven, Leuven, Belgium | [9]Institute of Ecology, Leuphana University of Lüneburg, Lüneburg, Germany | [10]Division of Ecology, Evolution and Biodiversity Conservation, KU Leuven, Leuven, Belgium | [11]Disturbance Ecology and Vegetation Dynamics, Bayreuth Center of Ecology and Environmental Research (BayCEER), University of Bayreuth, Bayreuth, Germany | [12]Department of Invasion Ecology, Institute of Botany, Czech Academy of Sciences, Prague, Czech Republic | [13]Faculty of Environmental Sciences, Czech University of Life Sciences Prague, Prague, Czech Republic | [14]UMR CNRS 7058 'Ecologie et Dynamique des Systèmes Anthropisés' (EDYSAN), Université de Picardie Jules Verne, Amiens, France | [15]Institute of Biology/Geobotany and Botanical Garden, Martin Luther University Halle-Wittenberg, Halle, Germany | [16]Department of Land Resources and Environmental Sciences, Montana State University, Bozeman, Montana, USA | [17]Ecology & Biodiversity, Department of Biology, Utrecht University, Utrecht, the Netherlands

Correspondence: Renée Lejeune (reneelejeune@hotmail.be)

Received: 1 September 2025 | **Revised:** 23 March 2026 | **Accepted:** 2 April 2026

Handling Editor: Bonnie Waring

ABSTRACT

Aim: Mountain roads host plant communities that differ strongly from the adjacent natural vegetation. Besides the effect of propagule pressure, altered disturbance and soil processes, one of the reasons given for the strong influence of mountain roads on species distributions is a significantly altered soil thermal microclimate in the roadside compared to the adjacent vegetation, as a direct consequence of road disturbance. However, the thermal microclimatic differences between roadside and natural vegetation have rarely been quantified, particularly across large spatial extents. This study provides the first global quantification of roadside soil temperature patterns along elevational gradients.

Location: Mountain roads in eight mountain regions from the Mountain Invasion Research Network (MIREN): Argentina, Chile, Czech Republic, Norway, Spain (Tenerife and La Palma), Switzerland, and the USA.

Methods: In this study, we analysed in situ measured topsoil temperatures (< 10 cm) and forest cover of roadsides and adjacent natural vegetation plots, in a systematically paired design.

Results: Across most regions, roadside soils exhibited consistently warmer maxima (3.62°C ± 2.61°C) and colder minima (1.39°C ± 1.40°C) than soils in adjacent vegetation. Although temperature distributions between roadside and natural habitats largely overlapped, these systematic shifts indicate increased thermal variability and higher frost risk in roadside environments.

Main Conclusions: Roadsides create distinct thermal microhabitats even within heterogeneous mountain landscapes. These altered temperature regimes, particularly when combined with vegetation structure and other environmental factors such as soil

This is an open access article under the terms of the Creative Commons Attribution License, which permits use, distribution and reproduction in any medium, provided the original work is properly cited.

© 2026 The Author(s). *Global Ecology and Biogeography* published by John Wiley & Sons Ltd.

moisture, may influence plant performance and distribution. Our findings highlight the ecological relevance of thermal microclimates in understanding biodiversity patterns along mountain roads.

1 | Introduction

Both the effects of mountain roads and the elevation-dependent temperature gradient on plant communities in mountain ecosystems are well understood. Plant communities along mountain roads are known to significantly differ from those in the surrounding natural vegetation (Seipel et al. 2012; Haider et al. 2018). Indeed, both native and non-native species reportedly shift their distributions along mountain roads, expanding their range limits (Lembrechts et al. 2017; Iseli et al. 2023). These changes in communities have been linked to a diverse range of factors, including facilitated propagule transportation, a higher intensity and frequency of disturbance regimes, altered biotic interactions, and modified soil conditions compared to the adjacent vegetation (Rauschert et al. 2017; Müllerová et al. 2011). Plant communities along elevational gradients are expected to shift upslope in response to climate warming (Mountain Research Initiative EDW Working group 2015) and amplified microclimatic fluctuations along mountain roads may further enhance this effect compared to adjacent, less disturbed vegetation. However, the nature of the latter, and the magnitude of these microclimatic differences between roadside and adjacent natural vegetation, have rarely been quantified (but see e.g., Delgado et al. 2007 for mountain forests on Tenerife) and surely not globally across multiple sites, hampering assessment of their broader importance.

Microclimate is inherently multidimensional, emerging from non-linear interactions among radiation, soil moisture, humidity, snow cover, and temperature. While we focus here on soil thermal microclimate, temperature represents a central and integrative component of microclimatic conditions and strongly influences ecological processes. Previous research shows that roadsides can significantly alter microclimatic environments (Delgado et al. 2007), and soil-level temperatures have been shown to be more extreme (i.e., higher maxima, lower minima) when vegetation cover is reduced due to either natural or human-induced disturbances (Spellerberg 1998; Lembrechts et al. 2018; Haesen et al. 2023). These patterns are well known for lowland forests (De Frenne et al. 2021).

In alpine systems, however, effects may differ. Vegetation is typically shorter and less dense, so disturbances may cause smaller relative reductions in structural buffering capacity (Lembrechts et al. 2014), rendering a relatively smaller reduction in the buffering capacity of vegetation cover. Additionally, the more complex topography and thus topoclimatic heterogeneity in mountains might obscure any general trend. Finally, microclimate temperatures in mountain soils are in general, for at least some part of the year, defined by snow cover (Rixen et al. 2022). Snow cover along roads may be reduced through human practices (snow removal, salt application) as well as through natural processes (higher solar radiation, wind) lowering winter soil temperatures because of the missing isolating effect of snow (Freppaz et al. 2008; Harder et al. 2020), and earlier spring onset (Koivusalo and Kokkonen 2002). Conversely, snow may accumulate along road verges when blown or ploughed off the road (Semádeni-Davies 1999), buffering winter temperatures, increasing soil moisture and delaying spring onset (Pomeroy and Brun 2001; Pomeroy et al. 2001). The netto effect of snow on roadside thermal microclimate is thus uncertain.

Here, we present the first multiregional analysis of soil temperatures as a proxy for microclimate along mountain roads, utilizing in situ measurements from eight mountain regions around the world. We hypothesise that (1) roadside soil temperatures will significantly differ from those in adjacent vegetation, with notably higher maximum and summer soil temperatures due to increased solar exposure. Given the expected heterogeneity in snow patterns, we further hypothesise that (2) mean and minimum winter soil temperatures on roadsides will vary relative to adjacent vegetation, depending on both roadside management practices and regional snow conditions; for example, snow removal is expected to lower winter minima, whereas snow accumulation may buffer temperatures. Consequently, as a result of increased summer maxima (on average, a positive effect on growing season temperatures) and high winter temperature variability (on average, a neutral effect on growing season temperatures), we predict (3) a greater number of growing degree days (GDDs) and higher mean annual soil temperatures in roadsides. All effects are expected to be (4) more pronounced at low than at high elevations for maximum temperatures due to the more substantial impact of roadside disturbances on vegetation cover and the negative correlation between elevation and vegetation cover and height (Lembrechts et al. 2014), yet potentially more pronounced at high elevations for minimum temperatures due to a stronger impact of snow at high elevations.

2 | Methods

2.1 | Field Monitoring

Temperatures were monitored in the topsoil layer (< 10 cm) of roadsides and adjacent natural vegetation plots, in a systematically paired design, along mountain roads in eight mountain regions from the Mountain Invasion Research Network (MIREN): Argentina, Chile, Czech Republic, Norway, Spain (Tenerife and La Palma), Switzerland, and the USA (Figure 1; Haider et al. 2022).

Within the framework of the long-term vegetation monitoring program directed by the MIREN network (www.mountaininvasions.org; Haider et al. 2022) along mountain roads (i.e., paved or gravel roads open to motorised vehicles), each region selected up to three roads that extend over a broad elevational gradient, from the bottom of the mountain region, in a valley, at sea level, or where no further elevation change occurred, whenever possible up till the highest elevation reached by roads in the region. The elevation gradient of each road was then divided into 19 equally wide elevational bands from the lowest to the highest possible sampling location, resulting in a total of 20 sample sites per road. At each of these sample sites, three 2 m × 50 m vegetation survey plots were laid out in the form of a 'T'-shaped transect, one plot parallel to the road and the other two extending

14668238, 2026, 4, Downloaded from https://onlinelibrary.wiley.com/doi/10.1111/geb.70237 by Eduardo Fuentes-Lillo - Universidad De Concepcion , Wiley Online Library on [04/05/2026]. See the Terms and Conditions (https://onlinelibrary.wiley.com/terms-and-conditions) on Wiley Online Library for rules of use; OA articles are governed by the applicable Creative Commons License

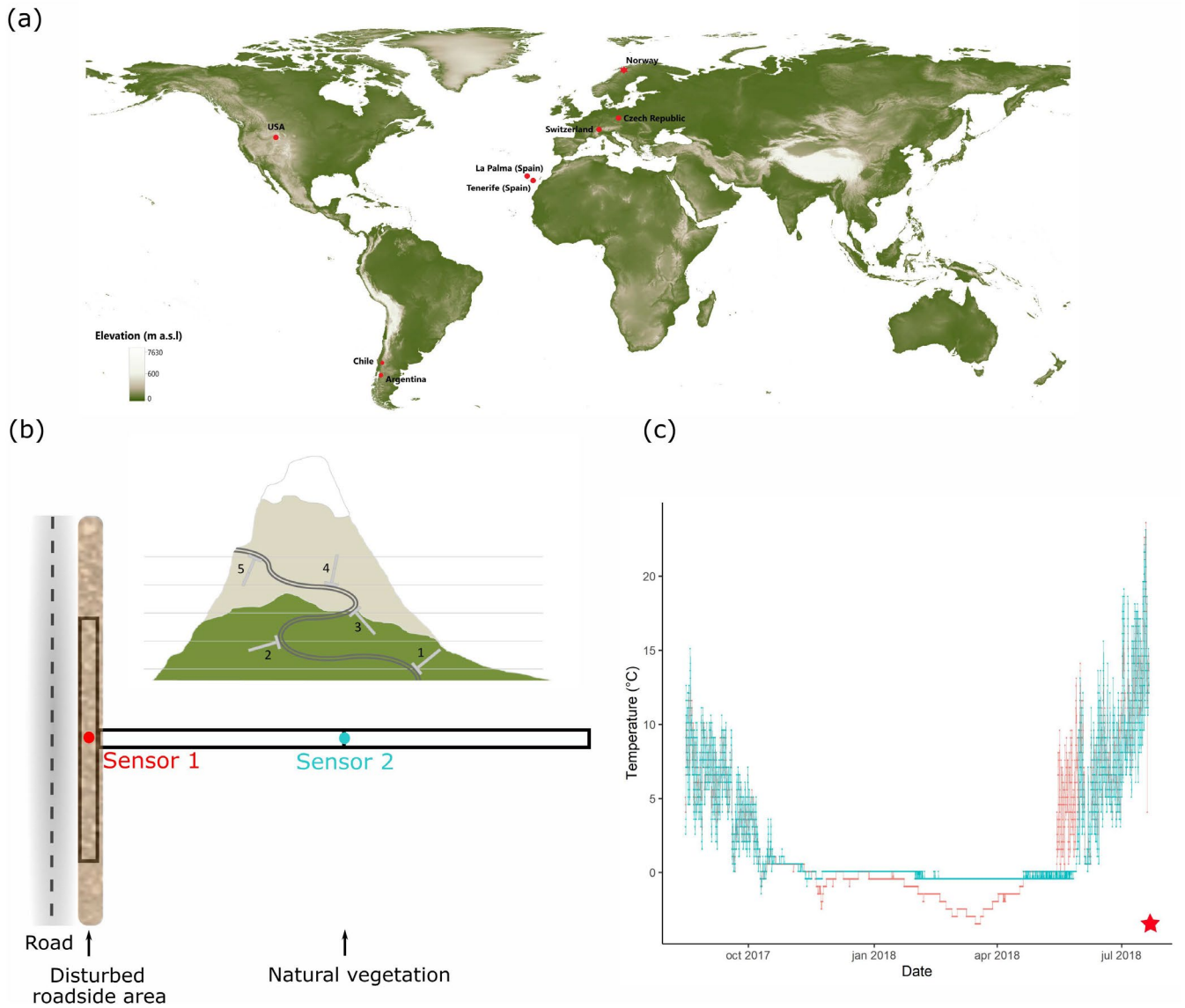

FIGURE 1 | (a) Location of the eight study regions across the globe, on a backdrop of a digital elevation model highlighting high-elevation zones (Tachikawa et al. 2011). Naming convention of regions is following Haider et al. (2022). (b) MIREN transect design showing a T-shaped transect bordering one roadside along an elevational gradient, as well as the location of the two soil temperature sensors in each transect, along the roadside (sensor 1) and within adjacent and undisturbed vegetation (sensor 2) (adapted from Haider et al. 2022). The inset mountain drawing shows the spread of T-transects along a hypothetical mountain road. (c) Example of a one-year temperature time series, at hourly resolution, in a roadside (red) and adjacent vegetation (blue) plot, based on data from a plot at 500 m a.s.l. in Norway (★). Note the quasi-horizontal line during winter in the adjacent vegetation, indicating the insulating effect of snow.

end-to-end and perpendicular to the road, starting from the center of the first plot, with midpoints at 25 and 75 m from the roadside plot (Figure 1b; Haider et al. 2022).

In the eight regions, these T-shaped vegetation plots have been installed between 2007 and 2021, with the intention of repeating vegetation monitoring every 5 years. In all or a selection of these vegetation plots, small, rugged temperature sensors (iButtons DS1921G or DS1922L (Maxim Integrated), HOBO Pendant UA-001-08 (Onset) or TOMST TMS4s (shortened; 23 cm instead of the standard 29 cm; Wild et al. 2019; Table 1)) were installed, each time pairwise: one sensor in the middle of the roadside plot vs. one in the middle of the second perpendicular plot (i.e., at 50 m from the roadside plot). One exception is Switzerland, where this pairwise design was not present. Paired sensors were of the same brand to rule out a possible effect of the factor brand. iButtons were wrapped in parafilm to prevent moisture damage and put into a small Ziplock bag; iButtons and HOBOs were buried just below the soil surface (0–5 cm). The shortened TOMST TMS4s sensors were installed vertically, with their top at the soil surface, and the data from the second sensor (6 cm below the soil surface) was used. Note that when measuring the temperature of soil below the surface, no radiative heat is supplied to a thermometer and the errors in measurement resulting from, for example, sensor brand or wrapping are likely to be negligible (Maclean et al. 2021). Sensors measured temperatures every 15 to 240 min over a period of at least 12 months between 2014 and 2022 (Table 1 and Figure 1). In all regions, plot-level forest cover was documented over the elevational gradient as the percentage of surface area covered by trees per T-transect.

14668238, 2026, 4, Downloaded from https://onlinelibrary.wiley.com/doi/10.1111/geb.70237 by Eduardo Fuentes-Lillo - Universidad De Concepcion , Wiley Online Library on [04/05/2026]. See the Terms and Conditions (https://onlinelibrary.wiley.com/terms-and-conditions) on Wiley Online Library for rules of use; OA articles are governed by the applicable Creative Commons License

TABLE 1 | Number of transects, number of sensors, start date and end date of soil temperature measurements, logger brand and type, measurement interval, and elevational range for all eight mountain regions.

	Number of transects	Number of sensors	Start date (month/year)	End date (month/year)	Logger brand	Logger type	Measurement interval (minutes)	Elevational range (m)
Norway	60	120	07/2014	07/2019	iButton HOBO	DS1921G (15%)[a] DS1922L (54%) UA-001-08 (31%)	240 90 60	13–1116
Czech Republic	5	10	06/2021	11/2022	TOMST	TMS4s	15	544–1400
Argentina	34	58	04/2017	05/2018	iButton	DS1922L	90	897–1678
USA	60	111	10/2015	06/2017	iButton	DS1922L	90	1803–3175
Switzerland	10	19	09/2017	10/2019	iButton	DS1922L	90	409–1805
Chile	60	120	04/2016	05/2017	iButton	DS1922L	90	274–1672
La Palma	32	39	03/2024	02/2025	TOMST	TMS4s	15	159–2282
Tenerife (Spain)	60	113	02/2018	05/2019	HOBO	UA-001-08	90	24–2377

Note: Regions here and throughout are ordered from low to high mean annual soil temperature in their lowest elevation plot.
[a]Percentages of the total amount of sensor-years in case multiple sensor types were used over the 5 years measurement period.

2.2 | Temperature-Related Bioclimatic Variables

The sensor data was used to calculate a series of temperature-related bioclimatic variables for each location: (i) mean annual temperature (averages over a 12-month period; BIO1 following the ANUCLIM framework, Xu and Hutchinson 2011); (ii) mean summer (BIO10) and (iii) winter (BIO11) temperature (average over, respectively, July–September for summer and December–February for winter in the Northern Hemisphere, and vice versa in the Southern Hemisphere; these months were in each region identified as the warmest and coldest quarter based on the available data); and (iv) growing degree days (GDD, in °C × days), representing the sum of all daily mean temperatures in a year that exceed a specific threshold, set here at 0°C. Although not part of the ANUCLIM framework, GDD provides ecologically meaningful insights into the impacts of temperature variation across spring, summer, and autumn. Finally, we obtained (v) the maximum (BIO5) and (vi) the minimum (BIO6) temperature of the warmest and coldest months of the year, respectively. More precisely, BIO5 was calculated as the 5% highest daily maximum temperature in a month, to remove extreme outliers. Similarly, BIO6 was defined as the 5% lowest daily minimum in a month.

2.3 | Statistical Analysis

All analyses were performed in R version 4.2.1. Each bioclimatic variable, used as a response variable, was modelled as a function of plot-level elevation (in m a.s.l.) interacting with distance to the road (binary: roadside vs. 50 m distance from the roadside plot in adjacent natural vegetation). Additionally, each bioclimatic variable was modelled as a function of forest cover of the adjacent plot (in percentage) interacting with distance to the road. We used separate models due to the correlation between plot-level elevation and forest cover (see Supporting Information A). We modelled temperatures as a function of forest cover in the adjacent plot, assigning the same forest cover value to the roadside plot. This approach allowed the forest cover variable to reflect changes in forest cover across the elevation gradient, while the influence of roadside disturbance on soil thermal microclimate—via reduced forest cover, among others—was captured by the distance-to-road variable. This distinction enabled us to focus on the overall effect of roadside disturbance. Models were fitted using linear mixed-effects models (package *lme4*, Bates et al. 2015), with the elevation × distance to the road interaction as a random slope effect acting on region. This way, we could obtain region-specific coefficients for both the elevation and road parameter and their interaction term, using partial pooling (Harrison et al. 2018). In addition to that and to account for the paired sampling design, that is, two sensors sharing the same transect, we added a unique transect identifier or ID as a random intercept term in each model. This paired sampling design is similar for all sampled regions, therefore region and transect ID are treated as crossed random effects.

As temperature variation decreased near 0°C, six of the investigated bioclimatic variables (all except growing degree days) were log-transformed. To avoid taking the logarithm of the few negative values, we first rescaled each variable by adding a constant equal to 0.01-min(bio_variable), ensuring that all values were positive prior to transformation.

14668238, 2026, 4, Downloaded from https://onlinelibrary.wiley.com/doi/10.1111/geb.70237 by Eduardo Fuentes-Lillo - Universidad De Concepcion , Wiley Online Library on [04/05/2026]. See the Terms and Conditions (https://onlinelibrary.wiley.com/terms-and-conditions) on Wiley Online Library for rules of use; OA articles are governed by the applicable Creative Commons License

The final model thus had the form:

```
log(bio. variable + (0.01-min(bio. variable)) ~ Elevation × Road + (Elevation × Road | Region) + (1 | Transect ID)).
```

When presenting predicted response curves, we back-transformed model predictions to the original scale by exponentiating the fitted values and subtracting the same constant used for rescaling, that is,

```
predicted_original <- exp(predicted) - (0.01 - min(bio_variable))
```

All reported effect sizes and ecological interpretations are based on these back-transformed values, ensuring that results are expressed in the original temperature units.

Using the same data, an assessment of global emerging patterns was made for each bioclimatic variable to visualise the effect of both elevation and forest cover independent of the region. For this, a reduced version of the above-described model was used. Since the different regions had differing elevational ranges, elevation was scaled within each region, using a mean of zero and a standard deviation of one.

Model predictions were visualised using the *ggplot2* package (Wickham 2011).

We further performed a variance partitioning analysis to quantify the relative contribution of the main fixed effects and the random-effects structure. We calculated marginal and conditional R2 for mixed models following the Nakagawa framework using the performance package (Lüdecke et al. 2021). The unique (semi-partial) contribution of each focal fixed effect (i.e., elevation or forest cover, road, and their interaction) was estimated using a leave-one-out approach: for each term, we fitted a reduced model excluding that term and quantified the change in marginal R2 relative to the full model. Variance attributable to the random-effects structure (regional heterogeneity and transect-level differences) was summarised as the difference between conditional and marginal R2. Semi-partial R2 and variance partitioning were implemented using the partR2 package (Stoffel et al. 2021). This procedure allowed us to directly compare the relative explanatory power of elevation, forest cover, roadside position and site identity.

3 | Results

3.1 | Global Model

Across all regions, mean annual and mean summer soil temperatures, Growing Degree Days, and maximum annual soil temperatures were higher in roadsides compared to adjacent vegetation (Figure 2; Tables 2 and 3). Conversely, annual minimum and mean winter soil temperatures became lower in roadsides towards higher elevations. Elevation significantly influenced all temperature variables, often interacting with the road effect. For instance, mean summer soil temperatures on the roadsides were 1.79°C warmer than in adjacent vegetation at low elevations but only 1.07°C warmer at high elevations (Table 2).

The effect of forest cover on the temperature-related bioclimatic variables was significant for mean summer temperatures, Growing Degree Days and maximum annual soil temperatures. Most notably, for all variables, there was a positive interaction between distance to the road and forest cover: soil temperatures in roadsides were substantially higher relative to adjacent vegetation at sites with high forest cover compared to those with low forest cover (Tables S1 and S2; Figure S1).

3.2 | Regional Trends

At the regional level, soil temperature patterns on roadsides broadly reflect those observed in the global-level model, with notable regional variations (Figures 3 and 4; Tables 2 and 3). Mean annual soil temperatures were consistently higher on roadsides than adjacent vegetation in five out of eight regions. Roadside temperatures were, on average, 0.63°C ± 0.52°C higher in lowlands (lowest plot on transect) and 0.88°C ± 0.69°C higher in highlands (highest plot on transect) than in adjacent and undisturbed vegetation. Mean summer soil temperatures followed a similar trend, being consistently higher on roadsides across seven out of eight regions, on average 1.64°C ± 1.24°C than in adjacent vegetation. Mean winter soil temperatures, however, were lower on roadsides in four out of eight regions or became lower with elevation in two other regions, being 0.59°C ± 0.51°C lower, on average, than in adjacent vegetation (Figure 3 and Table 2).

Similarly, growing degree days (GDD) were consistently higher on roadsides than in adjacent vegetation in six out of eight regions, averaging 322.93°C ± 164.64°C × days higher across these regions, but became lower towards higher elevations in two regions (Figure 4 and Table 3). Annual soil temperature maxima were consistently higher on roadsides in seven regions increasing by up to 3.62°C ± 2.61°C, on average, while annual minima were consistently lower in two regions or became lower at higher elevations in four others, decreasing with 1.39°C ± 1.40°C on average. Importantly, while adjacent vegetation soil temperatures declined with elevation, roadside soil temperatures sometimes increased, such as for annual maxima in Norway, Switzerland, the USA and La Palma. In both Norway and Switzerland minimum annual soil temperatures seem to increase with elevation in roadsides as well as the adjacent vegetation. The USA showed the largest roadside-to-vegetation difference for annual maximum soil temperatures (Table 2).

The effect of forest cover, though not significant in all regions, revealed distinct trends where present. Mean annual soil temperatures increased with forest cover in two regions and summer soil temperatures increased with forest cover in only one of the eight regions (warming effect) but decreased in the other four (cooling effect, Figure S2 and Table S1). Roadside mean annual and summer soil temperatures consistently exceeded those in adjacent vegetation across all regions, except for the mean annual temperature in Argentina at low elevations. Mean annual soil temperatures were on average 0.47°C ± 0.29°C higher at low elevations and 1.36°C ± 1.13°C higher at high elevations.

14668238, 2026, 4, Downloaded from https://onlinelibrary.wiley.com/doi/10.1111/geb.70237 by Eduardo Fuentes-Lillo - Universidad De Concepcion , Wiley Online Library on [04/05/2026]. See the Terms and Conditions (https://onlinelibrary.wiley.com/terms-and-conditions) on Wiley Online Library for rules of use; OA articles are governed by the applicable Creative Commons License

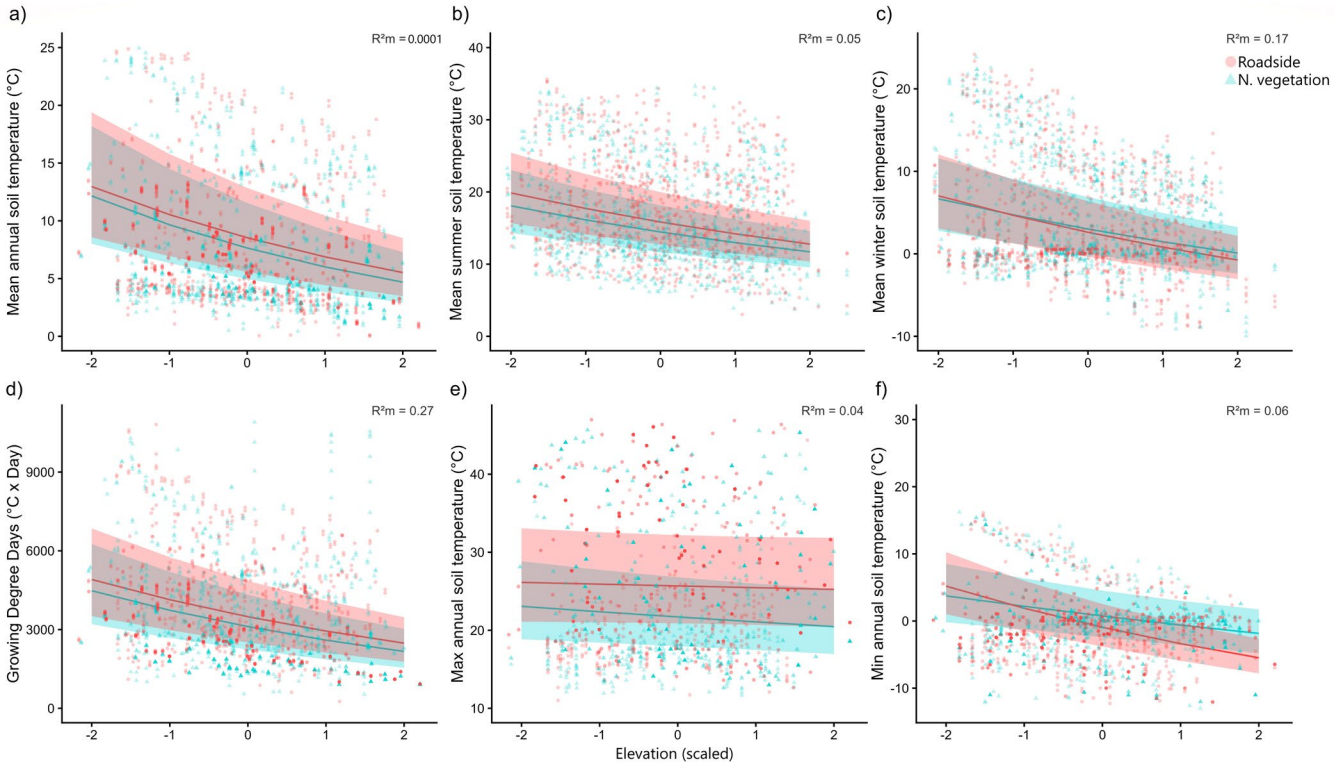

FIGURE 2 | Key temperature-related soil bioclimatic variables as a function of elevation (*x*-axis, elevational values scaled within each region with a mean of zero and a standard deviation of one) and distance to the road including the 95% confidence intervals (roadside = red, natural vegetation = blue) across all eight mountain regions. Top row: Mean annual soil temperature, monthly mean soil temperature during summer (July–September on the northern hemisphere, December–February on the southern hemisphere) and monthly mean soil temperature during winter (December–February on the northern hemisphere, July–September on the southern hemisphere). Bottom row: Growing Degree Days (GDDs), annual maximum soil temperature and annual minimum soil temperature. Points are raw measurements, fitted curves are drawn using the coefficients of the fixed effects of linear mixed models using the logarithm of the dependent variable (see Table 1).

Mean summer soil temperatures were 0.83°C ± 0.52°C higher at low elevations and 2.75°C ± 1.82°C higher at high elevations. There was a typical decrease with forest cover for GDD in six out of the eight regions, annual maximum temperatures in all regions, and minimum soil temperatures in six out of eight regions. Annual maximum soil temperatures were consistently higher or became higher with increasing forest cover on roadsides than in the adjacent, undisturbed vegetation. The same trend can be seen for GDD in seven out of eight regions (Table S2 and Figure S3). As with elevation, the USA showed the largest roadside-to-vegetation difference for annual maximum soil temperatures (Table S2).

3.3 | Variance Partitioning

While explanatory power is relatively low, elevation was for all bioclimatic variables—except maximum temperature—the parameter with the highest explanatory power (between 0.4% and 9.2%, Figure 5 and Table S3). In the models for forest cover, however, road was for all bioclimatic variables—except mean summer temperature—the parameter with the highest explanatory power (between 0.1% and 4.1%, Figure S4 and Table S4). As can be seen in Figure S5 for both the elevation and forest cover models, most of the variation in the random effect was captured by the regional level. One exception is mean annual soil temperature, where most of the variation was explained by the residuals.

4 | Discussion

Soil thermal microclimates in mountain roadsides differed consistently from those in adjacent natural vegetation, with average differences often exceeding 1°C. Although temperature distributions between roadside and natural habitats largely overlapped, these systematic shifts were substantial when placed in an elevational context. Indeed, roadside soil temperatures were frequently more similar to those observed several hundred meters higher or lower along the elevational gradient than to temperatures measured only 50 m away in adjacent vegetation at the same elevation. Our models estimated an average elevational lapse rate of 0.43°C per 100 m in soil temperature within natural vegetation, meaning that the observed 1°C roadside shift corresponds to more than 200 m of elevational displacement of the temperature regime. For comparison, the global macroclimatic lapse rate in air temperature is approximately 0.65°C per 100 m (ICAO 1993).

While we observed significant variation in these trends between regions, we especially found strong evidence for warmer annual maxima and summer mean soil temperatures along roadsides compared to the adjacent vegetation, and lower annual minima and mean winter soil temperatures on roadsides at high elevations. Looking at the forest cover gradient, the same patterns were found for annual maxima and summer soil temperatures, warmer along roadsides compared to the adjacent vegetation,

14668238, 2026, 4, Downloaded from https://onlinelibrary.wiley.com/doi/10.1111/geb.70237 by Eduardo Fuentes-Lillo - Universidad De Concepcion , Wiley Online Library on [04/05/2026]. See the Terms and Conditions (https://onlinelibrary.wiley.com/terms-and-conditions) on Wiley Online Library for rules of use; OA articles are governed by the applicable Creative Commons License

TABLE 2 | (a) Global coefficients (including *p*-values) and region-specific coefficients for key temperature-related soil bioclimatic variables as a function of elevation and distance to the road for eight mountain regions, as in Figure 2.

(a)					(b)	
					Roadside T relative to adjacent	
	Intercept	Elevation	Road	Elevation: Road	Lowland	Highland
Mean annual soil temperature (°C) -R^2C: 0.88 -R^2M: 0.10						
Global	**2.07 (< 0.001)**	**−0.22 (< 0.001)**	**0.10 (< 0.001)**	**0.020 (0.0964)**	**+0.81**	**+0.83**
Norway	1.62	−0.00052	0.13	−0.00014	+0.69	+0.11
Czech Republic	2.39	−0.00048	0.054	−0.0000091	+0.42	+0.23
Argentina	2.87	−0.00080	0.034	−0.000050	−0.10	−0.27
USA	4.5	−0.0012	−0.068	0.00011	+1.50	+0.67
Switzerland	2.69	−0.00032	0.0069	0.000052	+0.37	+0.87
Chile	2.90	−0.00040	−0.0045	0.000053	+0.17	+0.82
La Palma	3.03	−0.00023	−0.037	0.000063	−0.52	+1.38
Tenerife (Spain)	3.29	−0.00030	−0.047	0.000083	−1.18	+2.13
Mean summer soil temperature (°C) -R^2C: 0.81 -R^2M: 0.14						
Global	**2.43 (< 0.001)**	**−0.14 (< 0.001)**	**0.11 (< 0.001)**	**0.0009 (0.958)**	**+1.79**	**+1.07**
Norway	2.11	−0.00048	0.12	−0.000015	+0.90	+0.84
Czech Republic	2.68	−0.00042	0.03	0.000040	+0.50	+0.92
Argentina	2.80	−0.00047	−0.17	−0.00012	−0.60	+0.13
USA	3.87	−0.00075	0.68	−0.000178	+5.15	+0.39
Switzerland	2.86	−0.00024	0.08	0.000020	+1.15	+1.83
Chile	2.96	−0.00030	0.04	0.00050	+0.52	+2.05
La Palma	2.90	−0.00008	0.08	0.000007	+1.11	+2.23
Tenerife (Spain)	3.29	−0.00016	0.06	0.000028	+1.78	+2.43
Mean winter soil temperature (°C) -R^2C: 0.84 -R^2M: 0.17						
Global	**2.68 (< 0.001)**	**−0.11 (< 0.001)**	**−0.027 (0.009)**	**−0.024 (0.026)**	**+0.37**	**−0.85**
Norway	2.45	−0.00019	−0.041	−0.000020	−0.52	−0.48
Czech Republic	2.81	−0.00024	−0.049	−0.000004	−0.72	−0.41
Argentina	2.97	−0.00029	0.022	−0.000025	−0.030	−0.15
USA	3.40	−0.00047	0.338	−0.00017	+0.48	−1.28
Switzerland	2.79	−0.00018	−0.121	0.000038	−1.65	−0.39
Chile	3.18	−0.00029	0.013	−0.000011	+0.12	+0.013
La Palma	3.39	−0.00024	−0.039	0.000023	−1.23	+0.37
Tenerife (Spain)	3.49	−0.00028	0.027	−0.000006	+0.75	−0.24

Note: Top row: Mean annual soil temperature. Middle row: Monthly mean soil temperature during summer (July–September on the northern hemisphere, December–February on the southern hemisphere). Bottom row: Monthly mean soil temperature during winter (December–February on the northern hemisphere, July–September on the southern hemisphere). Coefficients are derived from a partial pooling procedure on linear mixed models using the logarithm of the dependent variable. Positive coefficients in black, negative coefficients in red. For 'road', positive values indicate a positive correlation between warming and closeness to the road. (b) Modelled thermal differences between the roadside and the adjacent at the lowest (lowland) and highest (highland) elevation of each region's elevational gradient. Negative differences (roadsides cooler than adjacent) in red. Regions are ordered from lowest to highest mean annual soil temperature in their lowest elevation plot. For each model, the conditional (R^2C) and marginal (R^2M) R^2 are given as well. Values derived from the global model are indicated in bold.

14668238, 2026, 4, Downloaded from https://onlinelibrary.wiley.com/doi/10.1111/geb.70237 by Eduardo Fuentes-Lillo - Universidad De Concepcion , Wiley Online Library on [04/05/2026]. See the Terms and Conditions (https://onlinelibrary.wiley.com/terms-and-conditions) on Wiley Online Library for rules of use; OA articles are governed by the applicable Creative Commons License

TABLE 3 | (a) Global coefficients (including *p*-values) and region-specific coefficients for key temperature-related soil bioclimatic variables as a function of elevation (m a.s.l.) and distance to the road (road versus adjacent) for eight mountain regions, as in Figure 3.

(a)					(b)	
					Roadside T relative to adjacent	
	Intercept	Elevation	Road	Elevation: Road	Lowland	Highland
Growing Degree Days (°C × days) -R^2C: 0.93 -R^2M: 0.27						
Global	**8.04 (< 0.001)**	**−0.18 (< 0.001)**	**0.11 (< 0.001)**	**0.011 (0.325)**	**+426.49**	**+316.38**
Norway	8.18	−0.00073	0.071	0.000194	+160.92	+539.00
Czech Republic	8.34	−0.00068	0.065	0.000025	+205.98	+168.07
Argentina	8.52	−0.00062	0.058	−0.000053	+24.72	−60.80
USA	8.73	−0.00052	0.050	0.000062	+425.54	+330.40
Switzerland	8.62	−0.00046	0.054	0.000043	+398.83	+340.39
Chile	8.75	−0.00043	0.049	−0.000004	+394.54	+139.70
La Palma	8.95	−0.00029	0.042	0.000009	+635.19	+136.58
Tenerife (Spain)	9.14	−0.00025	0.034	−0.000028	+857.57	−274.27
Maximum annual soil temperature (°C) -R^2C: 0.80 -R^2M: 0.044						
Global	**2.65 (< 0.001)**	**−0.046 (0.0148)**	**0.247 (< 0.001)**	**0.033 (0.029)**	**+3.08**	**+4.77**
Norway	2.21	−0.00010	0.113	0.00048	+1.18	+4.78
Czech Republic	2.32	−0.00010	0.116	0.00004	+1.37	+1.59
Argentina	2.51	−0.00010	0.110	−0.00012	+0.04	−0.86
USA	3.04	−0.00009	0.086	0.00013	+6.50	+9.75
Switzerland	2.92	−0.00009	0.091	0.00011	+2.61	+5.37
Chile	3.00	−0.00009	0.088	0.00005	+2.05	+3.08
La Palma	2.91	−0.00009	0.091	0.00011	+2.07	+6.05
Tenerife (Spain)	3.52	−0.00009	0.068	0.00005	+2.41	+5.50
Minimum annual soil temperature (°C) -R^2C: 0.81 -R^2M: 0.061						
Global	**2.96 (< 0.001)**	**−0.072 (< 0.001)**	**−0.091 (< 0.001)**	**−0.077 (< 0.001)**	**+1.46**	***−3.63***
Norway	2.63	0.000161	−0.043	−0.000096	−0.76	−1.49
Czech Republic	3.05	−0.000056	0.035	−0.000071	+0.36	−0.89
Argentina	3.04	−0.000054	0.100	−0.000111	+0.24	−1.18
USA	3.97	−0.000541	1.090	−0.000543	+3.39	−4.96
Switzerland	2.94	−0.0000002	−0.118	−0.000002	−1.75	−1.89
Chile	3.10	−0.000086	0.097	−0.000098	+1.40	−0.86
La Palma	3.60	−0.000348	−0.021	0.000058	−0.13	+0.66
Tenerife (Spain)	3.53	−0.000309	0.009	0.000027	−0.019	+0.41

Note: Top row: Growing Degree Days. Middle row: Annual maximum soil temperature (95% highest). Bottom row: Annual minimum soil temperature (5% lowest). Coefficients are derived from a partial pooling exercise on linear mixed models using the logarithm of the dependent variable. Positive coefficients in black, negative coefficients in red. (b) Modelled temperature differences between the roadside and the adjacent at the lowest (lowland) and highest (highland) elevation of each region's elevational gradient. Negative differences (roadsides cooler than adjacent) in red. Regions are ordered from lowest to highest mean annual soil temperature in their lowest elevation plot. For each model, the conditional (R^2C) and marginal (R^2M) R^2 are given as well. Values derived from the global model are indicated in bold.

although forest cover itself was a less strong predictor than elevation. Overall, these findings suggest a greater coupling between thermal macro- and microclimatic fluctuations along roadsides than in the adjacent vegetation, implying that the natural conditions are less susceptible to changes in thermal macroclimatic conditions with the vegetation cover potentially acting

14668238, 2026, 4, Downloaded from https://onlinelibrary.wiley.com/doi/10.1111/geb.70237 by Eduardo Fuentes-Lillo - Universidad De Concepcion , Wiley Online Library on [04/05/2026]. See the Terms and Conditions (https://onlinelibrary.wiley.com/terms-and-conditions) on Wiley Online Library for rules of use; OA articles are governed by the applicable Creative Commons License

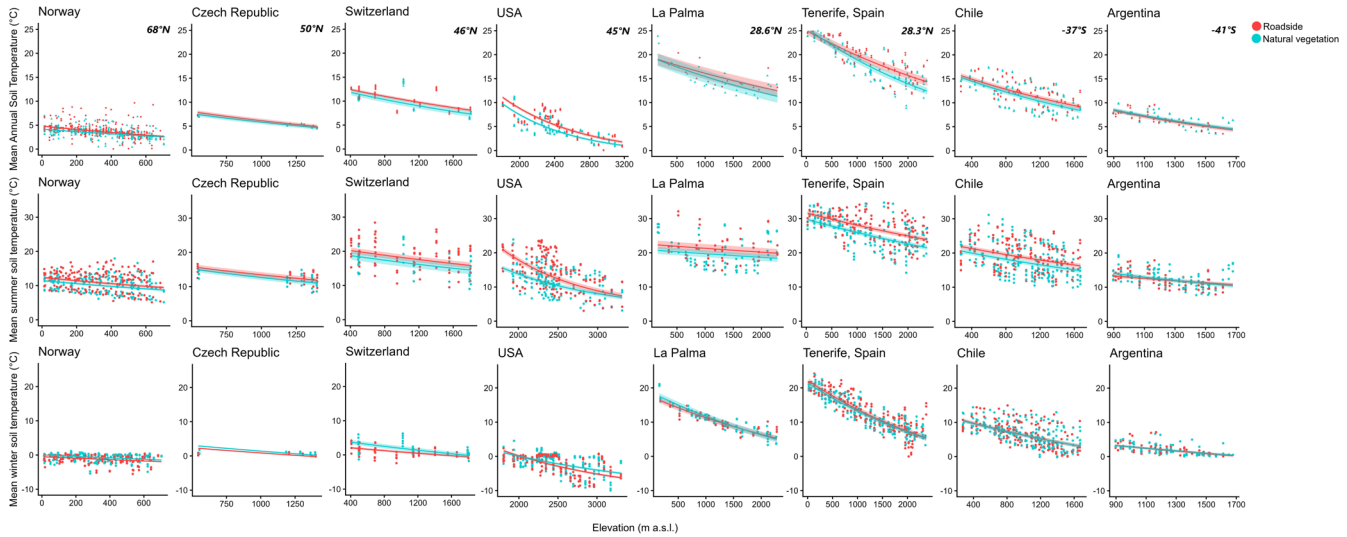

FIGURE 3 | Key temperature-related soil bioclimatic variables as a function of elevation (*x*-axis) and distance to the road including the 95% confidence intervals (roadside = red, natural vegetation = blue) for eight mountain regions. Top row: Mean annual soil temperature. Middle row: Monthly mean soil temperature during summer (July–September on the northern hemisphere, December–February on the southern hemisphere). Bottom row: Monthly mean soil temperature during winter (December–February on the northern hemisphere, July–September on the southern hemisphere). Points are raw measurements, fitted curves are from a partial pooling procedure using linear mixed-effects models with the logarithm of the dependent variable (see Table 1). Regions ordered from lowest to highest mean annual soil temperature in their lowest elevation plot.

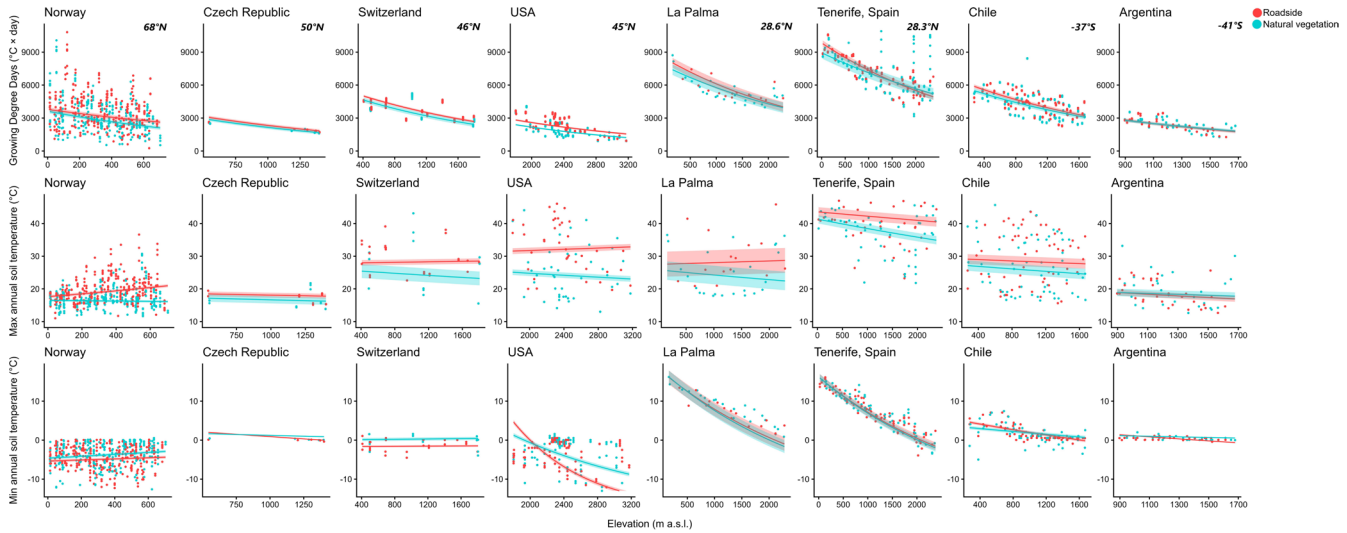

FIGURE 4 | Key temperature-related soil bioclimatic variables as a function of elevation (*x*-axis) and distance to the road including the 95% confidence intervals (roadside = red, natural vegetation = blue) for eight mountain regions. Top row: Growing Degree Days (GDDs). Middle row: Annual maximum soil temperature. Bottom row: Annual minimum soil temperature. Points are raw measurements, fitted curves are from a partial pooling exercise on linear mixed models using the logarithm of the dependent variable (see Table 2). Regions are ordered from lowest to highest mean annual soil temperature in their lowest elevation plot.

as a buffer. However, a potential amplifying effect of roadsides in comparison to temperature fluctuations as measured by regular weather stations cannot be ruled out.

As a result of the above, mean annual soil temperatures and GDDs were often higher on roadsides than in the adjacent vegetation. Noteworthy, the difference in GDD between roadside and natural communities was especially large at high forest cover, suggesting a substantial disruption of the well-known microclimate buffering capacity of forests (De Frenne et al. 2021). Roadside thermal microclimatic conditions could therefore be beneficial to species coming from warmer areas, in line with the observed significant upward shift in elevational distributions for both native and non-native lowland species along the roads in several of the studied mountain regions (Lembrechts et al. 2017; Iseli et al. 2023). While it is unlikely that these altered thermal microhabitat conditions are the only determinant of these elevational shifts upslope, it has been shown experimentally that locally increased GDDs are linked with improved establishment success of native

14668238, 2026, 4, Downloaded from https://onlinelibrary.wiley.com/doi/10.1111/geb.70237 by Eduardo Fuentes-Lillo - Universidad De Concepcion , Wiley Online Library on [04/05/2026]. See the Terms and Conditions (https://onlinelibrary.wiley.com/terms-and-conditions) on Wiley Online Library for rules of use; OA articles are governed by the applicable Creative Commons License

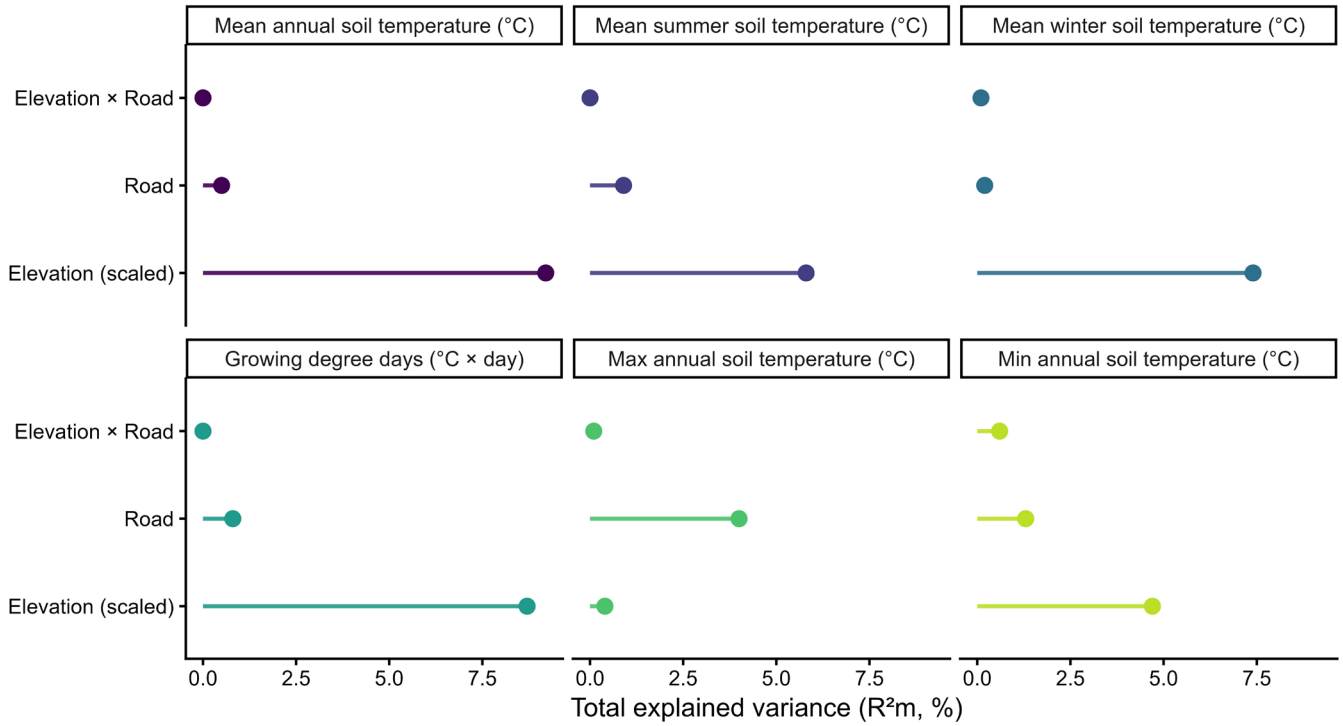

FIGURE 5 | Visual representation of the percentage of explanatory power of the fixed effects elevation (m a.s.l), distance to road and the interaction between both for each key temperature-related soil bioclimatic variable (see Table S3). Points show the total contribution of elevation (scaled), distance to road, and their interaction, calculated in partR2 as unique (semi-partial) + shared explained variance (shared reflects overlap among fixed-effect terms).

plant species above their current elevational distributions (Lembrechts et al. 2016, 2017, 2018). Importantly, however, these elevated roadside soil temperatures can, in combination with other environmental aspects linked to a warmer microclimate, also promote the establishment of non-native plant species near roadsides, as the warmer microclimate provides an important environmental variable for rapid growth, bypassing the cold adaptations required in alpine environments (Lembrechts et al. 2016, 2017, 2018).

As expected, roadside effects were more consistent for mean, summer, and maximum soil temperatures than for winter soil temperatures and minima. Winter temperature differences between roadsides and adjacent vegetation likely reflect variation in snow cover and snow depth across regions. Roads are often cleared of snow, whereas adjacent verges may accumulate snow due to wind redistribution or mechanical ploughing (Semádeni-Davies 1999), though snow clearing is typically restricted to lower elevations. Despite this complexity, winter soil temperatures and minima were shown to be more often lower on roadsides than in the adjacent vegetation, suggesting that snow cover loss is a more important process than snow accumulation, at least along the studied roads. This would be in line with the often-observed higher GDDs along roadsides, which could at least partially result from earlier snowmelt in spring (Wipf et al. 2006). Clearly, this earlier snowmelt causes a reduction of the albedo along roadsides in snow conditions which leads to a higher intake of radiative heat from the sun. This seemingly apparent role of snow is further supported by the fact that in study regions with the coldest climates, such as Norway and the USA, winter temperatures were consistently lower in the roadside than in the adjacent vegetation. That pattern was clearly reversed in the warmer climate of Tenerife, especially at low elevations, where snow never occurs.

The observed lower minima and winter soil temperatures in roadsides compared to the adjacent vegetation could at first glance be considered the drivers of the observed downward shifts, along mountain roads, of native plant species from high elevations (Lembrechts et al. 2017). It is however unlikely these range shifts are merely caused by thermal differences, as other microclimatic aspects like hydric conditions might play an equally important role. Nevertheless, most high elevation species are not limited by climate at the trailing edge of their distribution, yet by biotic interactions with more competitive lowland species (Boulangeat et al. 2012). It is thus more likely that the reduced vegetation cover in mountain roads, and the increased propagule transport along the roadside corridor are driving these downward shifts (Lembrechts et al. 2017). Additionally, the lower minima and thus increased frost risks in roadside soils did not stop the observed upward expansion of lowland species, suggesting that the increase of 1.64°C, on average, in mean summer soil temperatures and the increase of 322.93°C x days, on average, in GDD outweighed the 0.59°C drop, on average, in mean winter soil temperatures.

This increase in mean summer soil temperature and GDD associated with roadsides may, in combination with changes in other microclimatic dimensions, lead to significant shifts in phenology and functional diversity within roadside plant communities. Seed germination, for example, which is easily influenced by changes in thermal and hydric microclimatic conditions,

14668238, 2026, 4, Downloaded from https://onlinelibrary.wiley.com/doi/10.1111/geb.70237 by Eduardo Fuentes-Lillo - Universidad De Concepcion , Wiley Online Library on [04/05/2026]. See the Terms and Conditions (https://onlinelibrary.wiley.com/terms-and-conditions) on Wiley Online Library for rules of use; OA articles are governed by the applicable Creative Commons License

can occur earlier in warmer conditions, eventually leading to an advanced onset of flowering. While this might favor some species, it can disrupt many cold-adapted species with strict germination requirements (Espinosa del Alba et al. 2025). Microclimatic diversity is an important driver for intraspecific trait variation (ITV), a plastic response that allows plants to adjust to climatic changes, resulting in trait variation within the same species across warmer and colder habitats (Kemppinen and Niitynen 2022). Of course, thermal microclimate alone cannot be used to predict microclimate-driven ecological effects without accounting for other dimensions of microclimate such as soil moisture, radiation, or humidity. Nevertheless, our study should serve as a strong indicator that roadside effects on abiotic conditions are significant and thus hold potential downstream ecological effects.

Interestingly, local adiabatic lapse rates were often less steep for annual maximum soil temperatures on the roadside than in the natural vegetation, resulting in higher positive offsets in soil temperatures on the roadsides at higher than at low elevations. This was contrary to our expectations, yet might result from a strong shading at both low and high elevation in the adjacent vegetation while on the roadside there is strong shading only at low elevation. At high elevations, however, the adjacent vegetation is often of too short stature to shade disturbed roadsides, and its shading effect is thus limited to the soil growing right underneath it, so the intrinsically colder (i.e., high-elevation) sites would warm more (in summer). This would reduce the temperature gradient, hence the lapse rate. For mean winter temperatures, differences between roadside and adjacent vegetation were as expected often larger at high elevations, potentially due to larger differences in snow cover.

Patterns were largely but not entirely consistent between regions, showing that the impact of roads on thermal microclimate cannot simply be generalised across the globe. The low marginal R^2 values suggest that the main predictors, elevation and distance to the road, explain only a portion of the observed variance, with much variation arising from regional differences. This finding is supported by the results from the variance partitioning, where the region had the highest explanatory power. Part of these regional idiosyncrasies could be attributed to macroclimatic conditions in the region, as already shown above for mean winter temperatures, but can also be caused by differences in roadside management, such as the mowing regime, between regions.

For example, in Argentina, roadside soils exhibited unusually low mean annual and summer temperatures compared to adjacent vegetation, possibly due to tree plantings along roadsides in an otherwise short-grass landscape. Similarly, on La Palma and Tenerife, mean annual temperatures at low elevations were higher in adjacent vegetation than in roadside soils, likely reflecting a combination of very low forest cover and the high heat storage capacity of the volcanic bedrock (García-Alvarado et al. 2024; Gunerhan and Hepbasli 2005). Additionally, some high-elevation roads remain open during snowfall while others are closed, with varying snow accumulation on the roadsides, further contributing to regional variation. In Argentina, the absence of detailed forest cover data introduces additional uncertainty in interpreting these patterns.

Finally, it is important to take into account the temporal coverage of the dataset. Many regions are only represented by a single annual cycle and therefore do not capture interannual variability in weather conditions. The different regions are not all monitored during the same years; the observed regional idiosyncrasies might therefore also result from interannual variabilities. However, since most regions are positioned at great distances from each other, this effect will not be strong, and regions at smaller distances from each other clearly show a stronger consistency in patterns.

5 | Conclusions and Implications

Our results undeniably show the importance of roadsides creating different thermal microclimate conditions in otherwise heterogeneous mountain environments. In most regions, roadside soil temperatures had warmer and colder extremes than the adjacent vegetation, with lower cold extremes in winter and higher risks of extreme heat during summer, but roadsides had also longer growing seasons. These temperature trends could potentially explain some of the observed substantial upward shifts in lowland native and non-native species distributions along mountain roads (Lembrechts et al. 2016). Thermal microclimate may allow species to survive and reproduce in unsuitable macroclimate and adapt to climate change (Ackerly et al. 2020). Therefore, it can play an essential role in species distribution (Kemppinen et al. 2023). However, our understanding of potential species redistributions with climate change will also depend on other dimensions of microclimate that were not discussed in this research.

While our study focuses exclusively on thermal microclimate, it highlights the pioneering nature of globally coordinated roadside microclimate research. Future studies should aim to incorporate additional microclimatic variables such as soil moisture, radiation, and humidity, alongside land-use effects, to fully capture the environmental conditions influencing species distributions. Incorporating such high-resolution microclimatic data into large-scale biodiversity assessments will be essential to understanding how localised roadside effects interact with climate change to shape species redistributions over space and time (Lembrechts and Nijs 2020; De Frenne et al. 2021).

Acknowledgements

This research has been funded by the Research Foundation Flanders (12P1819N, G018919N and 1512720N) and BiodivERsA+-projects ASICS (G0H6720N, BiodivERsA+, BiodivClim call 2019–2020) and Forest-Web-3.0 (G0GDZ23N, BiodivERsA+, BiodivClim call 2023). A.P. and E.F.-L. acknowledge funding by Fondecyt 1180205, Fondecyt 1231616, ART 210038 and ANID/BASAL FB210006. Stef Haesen was supported by a FLOF fellowship (project nr. 3E190655) of the KU Leuven. M.V., J.P. and J.K. gratefully acknowledge the support of BiodivClim Call 2019 (TACR SS70010001) and long-term research development project RVO 67985939 (Czech Academy of Sciences).

Funding

This work was supported by Fonds Wetenschappelijk Onderzoek., Biodiversa+, Forest-Web-3.0 (Biodiversa+).

14668238, 2026, 4, Downloaded from https://onlinelibrary.wiley.com/doi/10.1111/geb.70237 by Eduardo Fuentes-Lillo - Universidad De Concepcion , Wiley Online Library on [04/05/2026]. See the Terms and Conditions (https://onlinelibrary.wiley.com/terms-and-conditions) on Wiley Online Library for rules of use; OA articles are governed by the applicable Creative Commons License

Conflicts of Interest

The authors declare no conflicts of interest.

Data Availability Statement

The data and code that supports the findings of this study are available in the Supporting Information of this article.

References

Ackerly, D. D., M. M. Kling, M. L. Clark, et al. 2020. "Topoclimates, Refugia, and Biotic Responses to Climate Change." *Frontiers in Ecology and the Environment* 18: 288–297.

Bates, D., M. Mächler, B. Bolker, and S. Walker. 2015. "Fitting Linear Mixed-Effects Models Using lme4." *Journal of Statistical Software* 67, no. 1: 1–48.

Boulangeat, I., D. Gravel, and W. Thuiller. 2012. "Accounting for Dispersal and Biotic Interactions to Disentangle the Drivers of Species Distributions and Their Abundances." *Ecology Letters* 15, no. 6: 584–593.

De Frenne, P., J. Lenoir, M. Luoto, et al. 2021. "Forest Microclimates and Climate Change: Importance, Drivers and Future Research Agenda." *Global Change Biology* 27, no. 11: 2279–2297.

Delgado, J. D., N. L. Arroyo, J. R. Arévalo, and J. M. Fernández-Palacios. 2007. "Edge Effects of Roads on Temperature, Light, Canopy Cover, and Canopy Height in Laurel and Pine Forests (Tenerife, Canary Islands)." *Landscape and Urban Planning* 81, no. 4: 328–340.

Espinosa del Alba, C., E. Fernández-Pascual, and B. Jiménez-Alfaro. 2025. "Microclimatic Variation Regulates Seed Germination Phenology in Alpine Plant Communities." *Journal of Ecology* 113: 249–262.

Freppaz, M., L. Celi, M. Marchelli, and E. Zanini. 2008. "Snow Removal and Its Influence on Temperature and N Dynamics in Alpine Soils (Vallee D'aoste, Northwest Italy)." *Journal of Plant Nutrition and Soil Science* 171, no. 5: 672–680.

García-Alvarado, J. J., V. Bello-Rodríguez, J. M. González-Mancebo, et al. 2024. "Updating Knowledge of Vegetation Belts on a Complex Oceanic Island After 20 Years Under the Effect of Climate Change." *Biodiversity and Conservation* 33: 2441–2463. https://doi.org/10.1007/s10531-024-02864-3.

Gunerhan, H., and A. Hepbasli. 2005. "Utilization of Basalt Stone as a Sensible Heat Storage Material." *Energy Sources* 27, no. 14: 1357–1366. https://doi.org/10.1080/009083190523253.

Haesen, S., J. Lenoir, E. Gril, et al. 2023. "Microclimate Reveals the True Thermal Niche of Forest Plant Species." *Ecology Letters* 26, no. 12: 2043–2055.

Haider, S., C. Kueffer, H. Bruelheide, et al. 2018. "Mountain Roads and Non-Native Species Modify Elevational Patterns of Plant Diversity." *Global Ecology and Biogeography* 27, no. 6: 667–678.

Haider, S., J. J. Lembrechts, K. McDougall, et al. 2022. "Think Globally, Measure Locally: The MIREN Standardized Protocol for Monitoring Plant Species Distributions Along Elevation Gradients." *Ecology and Evolution* 12, no. 2: e8590.

Harder, P., J. W. Pomeroy, and W. D. Helgason. 2020. "Improving Sub-Canopy Snow Depth Mapping With Unmanned Aerial Vehicles: Lidar Versus Structure-From-Motion Techniques." *Cryosphere* 14, no. 6: 1919–1935.

Harrison, X. A., L. Donaldson, M. E. Correa-cano, et al. 2018. "A Brief Introduction to Mixed Effects Modelling and Multi-Model Inference in Ecology." *PeerJ* 6: e4794. https://doi.org/10.7717/peerj.4794.

ICAO. 1993. *Manual of the ICAO Standard Atmosphere (Extended to 80 Kilometres (262 500 Feet))*. 3rd ed. International Civil Aviation Organization.

Iseli, E., C. Chisholm, J. Lenoir, et al. 2023. "Rapid Upwards Spread of Non-Native Plants in Mountains Across Continents." *Nature Ecology & Evolution* 7: 405–413.

Kemppinen, J., J. J. Lembrechts, K. Van Meerbeek, et al. 2023. "Microclimate, an Important Part of Ecology and Biogeography." *Global Ecology and Biogeography* 33: 6.

Kemppinen, J., and P. Niitynen. 2022. "Microclimate Relationships of Intraspecific Trait Variation in Sub-Arctic Plants." *Nordic Society OIKOS* 2022: e09507.

Koivusalo, H., and T. Kokkonen. 2002. "Snow Processes in a Forest Clearing and in a Coniferous Forest." *Journal of Hydrology* 262, no. 1–4: 145–164.

Lembrechts, J. J., J. M. Alexander, L. A. Cavieres, et al. 2017. "Mountain Roads Shift Native and Non-Native Plant Species' Ranges." *Ecography* 40: 353–364.

Lembrechts, J. J., J. Lenoir, M. A. Nuñez, et al. 2018. "Microclimate Variability in Alpine Ecosystems as Stepping Stones for Non-Native Plant Establishment Above Their Current Elevational Limit." *Ecography* 41: 900–909.

Lembrechts, J. J., A. Milbau, and I. Nijs. 2014. "Alien Roadside Species More Easily Invade Alpine Than Lowland Plant Communities in a Subarctic Mountain Ecosystem." *PLoS One* 9, no. 2: e89664.

Lembrechts, J. J., and I. Nijs. 2020. "Microclimate Shifts in a Dynamic World." *Science* 368, no. 6492: 711–712.

Lembrechts, J. J., A. Pauchard, J. Lenoir, et al. 2016. "Disturbance is the Key to Plant Invasions in Cold Environments." *Proceedings of the National Academy of Sciences of the United States of America* 113, no. 49: 14061–14066. https://doi.org/10.1073/pnas.1608980113.

Lüdecke, D., M. S. Ben-Shachar, I. Patil, P. Waggoner, and D. Makowski. 2021. "Performance: An R Package for Assessment, Comparison and Testing of Statistical Models." *Journal of Open Source Software* 6, no. 60: 3139.

Maclean, I. M., J. P. Duffy, S. Haesen, et al. 2021. "On the Measurement of Microclimate." *Methods in Ecology and Evolution* 12, no. 8: 1397–1410.

Mountain Research Initiative EDW Working Group. 2015. "Elevation-Dependent Warming in Mountain Regions of the World." *Nature Climate Change* 5: 424–430. https://doi.org/10.1038/nclimate2563.

Müllerová, J., M. Vítková, and O. Vítek. 2011. "The Impacts of Road and Walking Trails Upon Adjacent Vegetation: Effects of Road Building Materials on Species Composition in a Nutrient Poor Environment." *Science of the Total Environment* 409, no. 19: 3839–3849.

Pomeroy, J. W., and E. Brun. 2001. "Physical Properties of Snow." In *Snow Ecology: An Interdisciplinary Examination of Snow-Covered Ecosystems*, vol. 45, 118. Cambride University Press.

Pomeroy, J. W., P. Höller, and P. Marsh. 2001. "Snow Vegetation Interactions: Issues for a New." In *Soil-Vegetation-Atmosphere Transfer Schemes and Large-Scale Hydrological Models: Proceedings of an International Symposium (Symposium S5) Held During the Sixth Scientific Assembly of the International Association of Hydrological Sciences (IAHS) at Maastricht, the Netherlands, From 18 to 27 July 2001* (No. 270), 299. IAHS.

Rauschert, E. S. J., D. A. Mortensen, and S. M. Bloser. 2017. "Human-Mediated Dispersal via Rural Road Maintenance Can Move Invasive Propagules." *Biological Invasions* 19: 2047–2058.

Rixen, C., T. T. Høye, P. Macek, et al. 2022. "Winters Are Changing: Snow Effects on Arctic and Alpine Tundra Ecosystems." *Arctic Science* 8, no. 3: 572–608.

Seipel, T., C. Kueffer, L. J. Rew, et al. 2012. "Processes at Multiple Scales Affect Richness and Similarity of Non-Native Plant Species in Mountains Around the World." *Global Ecology and Biogeography* 21, no. 2: 236–246.

14668238, 2026, 4, Downloaded from https://onlinelibrary.wiley.com/doi/10.1111/geb.70237 by Eduardo Fuentes-Lillo - Universidad De Concepcion , Wiley Online Library on [04/05/2026]. See the Terms and Conditions (https://onlinelibrary.wiley.com/terms-and-conditions) on Wiley Online Library for rules of use; OA articles are governed by the applicable Creative Commons License

Semádeni-Davies, A. F. 1999. "Snow Heterogeneity in Luleå, Sweden." *Urban Water* 1, no. 1: 39–47.

Spellerberg, I. A. N. 1998. "Ecological Effects of Roads and Traffic: A Literature Review." *Global Ecology & Biogeography Letters* 7, no. 5: 317–333.

Stoffel, M. A., S. Nakagawa, and H. Schielzeth. 2021. "partR2: Partitioning R2 in Generalized Linear Mixed Models." *PeerJ* 9: e11414.

Tachikawa, T., M. Hato, M. Kaku, and A. Iwasaki. 2011. "Characteristics of ASTER GDEM Version 2." In *2011 IEEE International Geoscience and Remote Sensing Symposium*, 3657–3660. IEEE.

Wickham, H. 2011. "ggplot2." *Wiley Interdisciplinary Reviews: Computational Statistics* 3, no. 2: 180–185.

Wild, J., M. Kopecký, M. Macek, M. Šanda, J. Jankovec, and T. Haase. 2019. "Climate at Ecologically Relevant Scales: A New Temperature and Soil Moisture Logger for Long-Term Microclimate Measurement." *Agricultural and Forest Meteorology* 268: 40–47.

Wipf, S., C. Rixen, and C. P. Mulder. 2006. "Advanced Snowmelt Causes Shift Towards Positive Neighbour Interactions in a Subarctic Tundra Community." *Global Change Biology* 12, no. 8: 1496–1506.

Xu, T., and M. Hutchinson. 2011. *ANUCLIM Version 6.1 User Guide*. Australian National University, Fenner School of Environment and Society.

Supporting Information

Additional supporting information can be found online in the Supporting Information section. **Data S1:** Final_annual_incl_LP_1. **Data S2:** Final_monthly_incl_LP_1. **Data S3:** final_script_elevation_forestcover. **Figure S1:** Key temperature-related soil bioclimatic variables as a function of forest cover (*x*-axis) and distance to the road including the 95% confidence intervals (roadside = red, natural vegetation = blue) across all eight mountain regions. Top row: mean annual soil temperature, monthly mean soil temperature during summer (July–September on the northern hemisphere, December–February on the southern hemisphere), monthly mean soil temperature during winter (December–February on the northern hemisphere, July–September on the southern hemisphere). Bottom row: Growing Degree Days (GDDs), annual maximum soil temperature and annual minimum soil temperature. Points are raw measurements, fitted curves are drawn using the coefficients of the fixed effects of linear mixed models using the logarithm of the dependent variable. **Figure S2:** Key temperature-related soil bioclimatic variables as a function of forest cover (*x*-axis) and distance to the road including the 95% confidence intervals (roadside = red, natural vegetation = blue) for eight mountain regions. Top row: mean annual soil temperature, middle row: monthly mean soil temperature during summer (July–September on the northern hemisphere, December–February on the southern hemisphere). Bottom row: monthly mean soil temperature during winter (December–February on the northern hemisphere, July–September on the southern hemisphere). Points are raw measurements, fitted curves are from a partial pooling procedure on linear mixed models using the logarithm of the dependent variable (see Table 1). Regions ordered from lowest to highest mean annual temperature in their lowest forest cover plot. **Table S1:** (a) Global coefficients (including *p*-values) and region-specific coefficients for key temperature-related soil bioclimatic variables as a function of forest cover and distance to the road for eight mountain regions, as in Figure S2. Top row: mean annual soil temperature, middle row: monthly mean soil temperature during summer (July–September on the northern hemisphere, December–February on the southern hemisphere). Bottom row: monthly mean soil temperature during winter (December–February on the northern hemisphere, July–September on the southern hemisphere). Coefficients are derived from a partial pooling procedure on linear mixed models using the logarithm of the dependent variable. Positive coefficients in black, negative coefficients in red. (b) Modelled temperature differences between the roadside and the adjacent at the lowest and highest coverage percentage of each region's forest cover gradient. Negative differences (roadsides cooler than adjacent) in red. Regions are ordered from lowest to highest mean annual temperature in their lowest forest cover plot. **Figure S3:** Key temperature-related soil bioclimatic variables as a function of forest cover (*x*-axis) and distance to the road including the 95% confidence intervals (roadside = red, natural vegetation = blue) for eight mountain regions. Top row: Growing Degree Days (GDDs), middle row: maximum annual soil temperature. Bottom row: minimum annual soil temperature. Points are raw measurements, fitted curves are from a partial pooling exercise on linear mixed models using the logarithm of the dependent variable (see Table S2). Regions are ordered from lowest to highest mean annual temperature in their lowest forest cover plot. **Table S2:** (a) Global coefficients (including *p*-values) and region-specific coefficients for key temperature-related soil bioclimatic variables as a function of forest cover (%) and distance to the road (road versus adjacent) for eight mountain regions, as in Figure S3. Top row: Growing Degree Days, middle row: annual maximum soil temperature (95% highest). Bottom row: annual minimum soil temperature (5% lowest). Coefficients are derived from a partial pooling exercise on linear mixed models using the logarithm of the dependent variable. Positive coefficients in black, negative coefficients in red. (b) Modelled temperature differences between the roadside and the adjacent at the lowest and highest coverage percentage of each region's forest cover gradient. Negative differences (roadsides cooler than adjacent) in red. Regions are ordered from lowest to highest mean annual temperature in their lowest forest cover plot. **Figure S4:** Visual representation of the percentage of explanatory power of the fixed effects elevation (m a.s.l), distance to road and the interaction between both for each key temperature-related soil bioclimatic variable (see Appendix Table S4). Points show the total contribution of forest cover, distance to road, and their interaction, calculated in partR2 as unique (semi-partial) + shared explained variance (shared reflects overlap among fixed-effect terms). **Figure S5:** Visual representation of the percentage of explanatory power of the random effects (region and transect) and the residual for each key temperature-related soil bioclimatic variable. **Table S3:** (a) focal fixed effects elevation (m a.s.l.), distance to the road and the interaction between elevation-road and their unique (semi-partial) contribution to the mixed model. The explanatory power of the fixed effects was calculated for each key temperature-related soil bioclimatic variable: mean annual soil temperature (MAST), mean summer soil temperature (MSST), mean winter soil temperature (MWST), minimum annual soil temperature (MinAST), maximum annual soil temperature (MaxAST) and Growing Degree Days (GDD). Factor indicates the variance explained by the focal variable only, 'shared' indicates the variance shared by the focal variable and the rest of the model, and 'other' indicates the variance explained by the model without the focal variable. The sum of Factor and Shared indicates the total variable as explained by the focal variable. (b) Proportional contribution of the random-effects structure (Region and Transect ID) and the residual to the total variance in each mixed model. Region reflects among-region heterogeneity, Transect ID captures site-level variation associated with the paired design, and the residual represents unexplained within-site variability. **Table S4:** (a) focal fixed effects forest cover (%), distance to the road and the interaction between forest cover-road and their unique (semi-partial) contribution to the mixed model. The explanatory power of the fixed effects was calculated for each key temperature-relatedl soil bioclimatic variable: mean annual soil temperature (MAST), mean summer soil temperature (MSST), mean winter soil temperature (MWST), minimum annual soil temperature (MinAST), maximum annual soil temperature (MaxAST) and Growing Degree Days (GDD). Factor indicates the variance explained by the focal variable only, 'shared' indicates the variance shared by the focal variable and the rest of the model, and 'other' indicates the variance explained by the model without the focal variable. The sum of Factor and Shared indicates the total variable as explained by the focal variable. (b) Proportional contribution of the random-effects structure (Region and Transect ID) and the residual to the total variance in each mixed model. Region reflects among-region heterogeneity, Transect ID captures site-level variation associated with the paired design, and the residual represents unexplained within-site variability.

14668238, 2026, 4, Downloaded from https://onlinelibrary.wiley.com/doi/10.1111/geb.70237 by Eduardo Fuentes-Lillo - Universidad De Concepcion , Wiley Online Library on [04/05/2026]. See the Terms and Conditions (https://onlinelibrary.wiley.com/terms-and-conditions) on Wiley Online Library for rules of use; OA articles are governed by the applicable Creative Commons License